Journal of Applied Fluid Mechanics, Vol. 18, No. 3, pp. 798-808, 2025.
Available online at www.jafmonline.net, ISSN 1735-3572, EISSN 1735-3645.
https://doi.org/10.47176/jafm.18.3.2874

Behavior of a Glycerol Aqueous Droplet Impacting a Thin Water Film

J. Zhu[1], B. Liu [2], J. Sheng[2], S. Zheng[1], T. Lu[1] and X. Chen[1†]

[1.] *Beijing University of Chemical Technology, Beijing 100029, China*
[2.] *Science and Technology on Space Physical Laboratory, Beijing 100076, China*

†*Corresponding Author Email: xchen@buct.edu.cn*

ABSTRACT

The dynamic behavior of a glycerol aqueous droplet impacting on a thin water film was experimentally investigated with a high-speed camera. Numerous splash behaviors with different impact velocities (2.0-4.5 m/s), liquid film thicknesses (140-700 μm) and glycerol solution concentrations (30 wt%, 60 wt% and 80 wt%) were statistically analyzed, and finally classified based on morphological features. The laser-induced fluorescence images illustrate that the prompt splash secondary droplets mainly originated from the thin water film, while the components of delayed splash secondary droplets came from both the glycerol aqueous droplet and the thin water film. The results show that increasing viscosity suppresses prompt splash, inhibits the crown expansion and accelerates the crown collapse, while decreasing droplet viscosity facilitates prompt splash. The decreasing film thickness promotes passive delayed splash and increases the crown height. A splash morphology regime map was presented based on Weber number, dimensionless film thickness and solution mass concentration, delineating a threshold between prompt splash and coalescence. It also found that the occurrence of crown lamella rupture is sensitive to the film thickness and *We*.

Article History

Received May 25, 2024
Revised August 15, 2024
Accepted September 21, 2024
Available online January 1, 2025

Keywords:

Droplet impact
Thin liquid film
Crown
Splash
Secondary droplet

1. INTRODUCTION

Droplet impacting thin liquid film is a ubiquitous phenomenon in many systems such as falling film desalination (Liang et al., 2021), steam separator (Zhang & Liu, 2020), ink-jet printing (Nikolopoulos et al., 2005; Ersoy & Eslamian, 2019), spray cooling (Lee & Lee, 2011; Okawa et al., 2021) and fuel injection in internal combustion engines (Bernard et al, 2020; Yeganehdoust et al., 2020; Okawa et al., 2022).

Cossali et al. (1997) experimentally investigated the splash with water and glycerol aqueous solution. They found that droplets with higher viscosity begin to detach from jets even during the crown collapsing period and pointed out that the viscosity plays a significant role in defining the splash morphology. Wang and Chen (2000) experimentally studied the impact of a 60% - 80% glycerol aqueous droplet on liquid film with δ=0.049~0.098 and found that the *We* threshold is insensitive to the film thickness but increases with viscosity. The *We* threshold is defined as the minimum *We* value necessary to cause splash for a droplet impacting onto a liquid film. A droplet impacting a pool (2~25 mm) focusing on central jet with water and HFE7100 (Methoxy-nonafluorobutane, $C_4F_9OCH_3$) was performed by Manzello and Yang (2002). They found that the *We* threshold for central jet breakup is independent of pool depth. Furthermore, Manzello and Yang (2002) observed that the impact dynamics of water in HFE7100 pool was drastically different from the water droplet impingement on a water pool. Rioboo et al. (2003) distinguished the threshold between the crown-splash (bowl-shape crown) and deposition-crown (delayed splash) with four high-viscosity fluids in the dimensionless film thickness range of 0.06-0.14. Experiments by Cossali et al. (2004) showed that the film thickness plays a weak role in crown and splash formation. Okawa et al. (2006) presented a splash threshold of $K=Oh^{-0.4}\cdot We \approx 2100$ for identifying the central jet breakup. Vander Wal et al. (2005) found that the prompt splash and delayed splash are depressed by the increasing liquid film and postponed by increasing viscosity. Motzkus et al. (2009) showed that the number of secondary droplets from splashing increases with the increase of impact velocity and decreases with the increase of viscosity. Guo et al. (2010) also found that a larger viscosity inhibits the occurrence of splash. Ersoy and Eslamian (2020) performed a top-view phenomenological study with dyed droplets and identified the crown evolution when droplet impacting thin liquid film (δ=0.045, 0.089) is quite different from that of a thicker film (δ =0.179, 0.268 and 0.446) and pool (δ=1.116

NOMENCLATURE

C_m	mass concentration	v	impact velocity
d_0	droplet diameter	We	Weber number, $We=\rho v^2 d_0/\sigma$
D_c^*	dimensionless crown diameter	We^*	equivalent Weber number
h	film thickness	***Greek symbols***	
H_c	crown height	δ	dimensionless liquid film thickness, $\delta=h/d_0$
H_c^*	dimensionless crown height, $H_c^*=H_c/d0$	κ	viscosity ratio between the film and droplet
K^*	dimensionless parameter for splash threshold	μ	dynamic viscosity, μPa·s
Oh	Ohnesorge number, $Oh=\mu/(d_0\sigma\rho)^{-2}$	ρ	density
t	time	σ	surface tension coefficient

and 1.768). Wu et al. (2020) investigated a silicon oil droplet impacting on thin film with δ=0.016~0.035 by stereoscopic shadowgraph method. The crown lamella bottom breakdown splashing was observed, which was attributed to over-stretching crown lamella resulting from faster radial velocity. Zhu et al. (2021) further classified the splash evolution based on δ=0.07~0.23 and proposed a threshold between prompt splash with delayed splash and prompt splash without delayed splash. Moreover, Zhu et al. (2021) found that the central jet development is strongly related to the prior splash morphology.

Weiss and Yarin (1999) conducted pioneering numerical research on the dynamics of droplet impact on a liquid film. They identified that the formation of neck jetting (prompt splash) and crown are attributed to the kinematic discontinuity present in the velocity distribution within the liquid. Also, Liang et al. (2013) found that the large pressure difference in the neck region greatly affects the jet formation by using CLSVOF (the coupled level set and volume of fluid method). With same method, Guo et al. (2014) found the higher impact velocity leads to an earlier prompt splash occurrence and more secondary droplets. Guo et al. (2016) studied a droplet impacting a thin film with MOF (moment of fluid) method and found that the crown consists of liquid from both the thin film and the droplet, but that the splashed droplets mainly came from the liquid film.

The impact of a droplet on another liquid film differs from that on an identical liquid film, leading to a broader range of phenomena. Chen et al. (2017) showed that a large *We* promotes the formation and splash while a large film viscosity suppresses the formation of a crown and splash for a miscible film. Geppert et al. (2017) experimentally observed hole formation in the crown when a dissolved two-component droplet impacting on the liquid film for δ<0.1. The crown shapes (V-shaped, cylindrical and truncated-cone) confirm that vorticity production induces changes in the crown wall, which affects the crown diameter and height. Thoroddsen et al. (2006) observed a bowl-shaped crown with thousands of holes formed on the lamella by Marangoni stresses when they used a viscous droplet to impact a thin ethanol film. Their team further found that the holes also form in lamella when a viscous droplet impacts a thin film with larger surface tension but where the Marangoni stress changes direction. Shaikh et al. (2018) experimentally studied the droplet impacting on thin immiscible oil film and found that the size of secondary droplets from delayed splash increases as *We* increased.

Based on the above review, more research is needed to further explore the droplet-film interactions involving different types of fluids. Therefore, we conducted a detailed study on the splashing morphology of a glycerol aqueous droplet impacting water film with different film concentrations and film thicknesses, classifying the various splashing regimes. A splash regime map based on *We*, δ, and C_m was obtained, and the thresholds distinguishing between prompt splash and coalescence were also provided.

2. EXPERIMENTAL APPARATUS

The experiments were performed on the optical platform shown in Fig. 1. A high-speed camera (SA-X2, Photron) with a micro-lens (105 mm f/2.8G, Nikkor) was used to capture the impact and splash behaviors. Prior to each experiment, the camera was focused on a standard

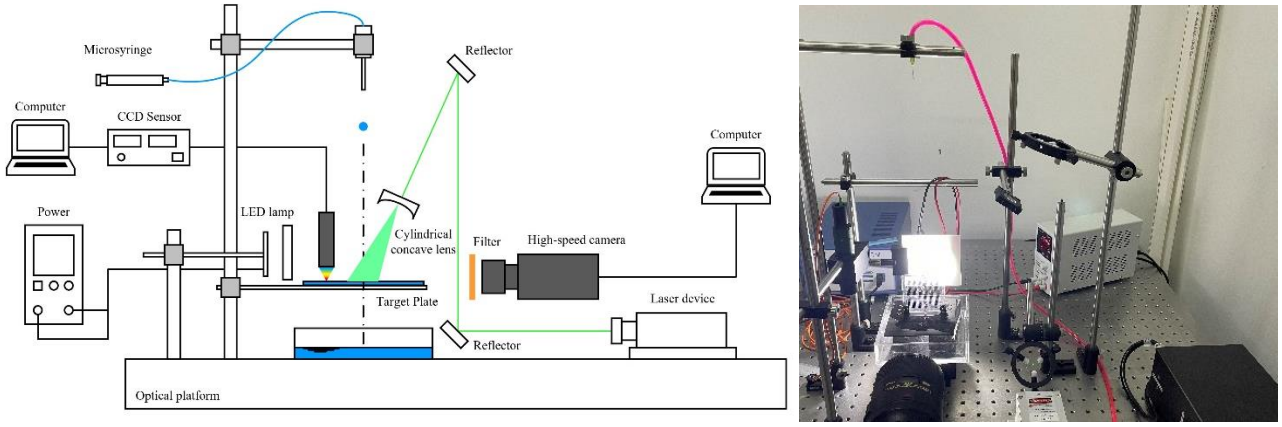

Fig. 1 Experimental system

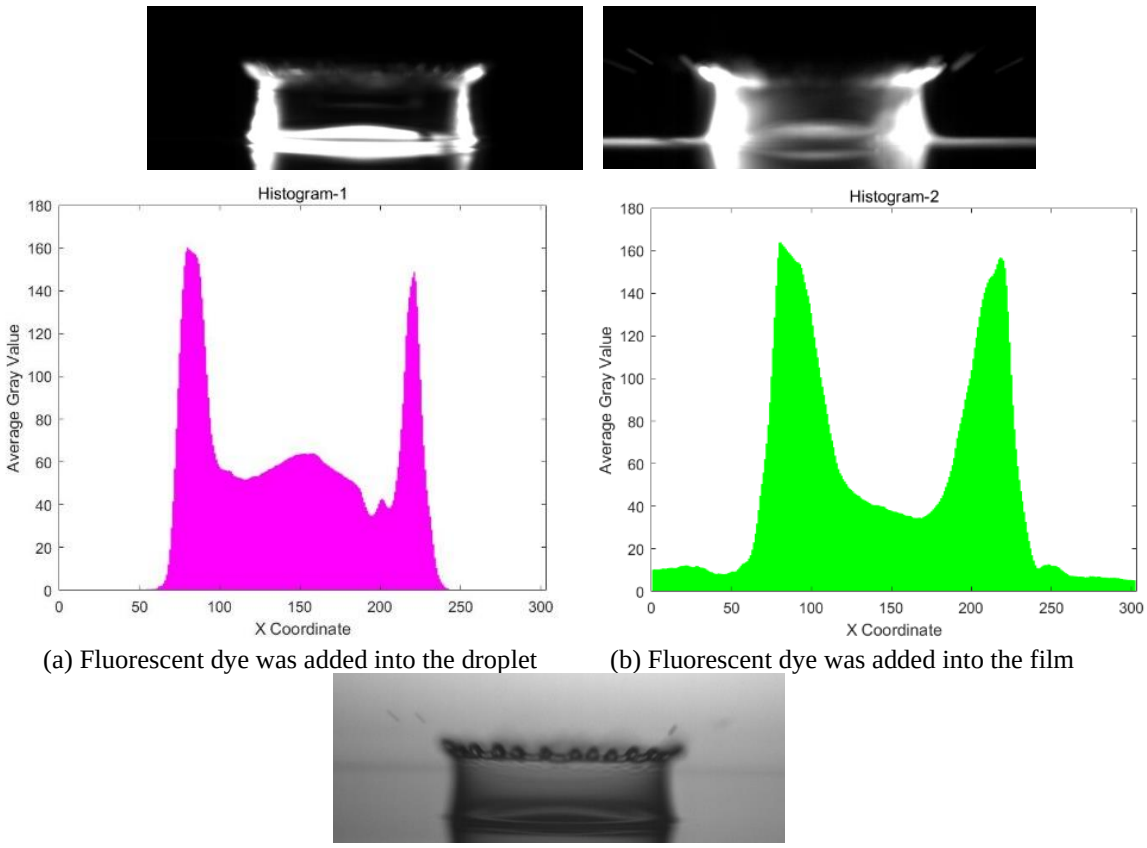

(a) Fluorescent dye was added into the droplet (b) Fluorescent dye was added into the film

(c) Back light

Fig. 2 Images obtained by PLIF and back light method (C_m = 60 wt%, δ=0.12 and *We*=503)

Table 1 Experiment Parameters

d_0, mm	h, μm	v, m/s
1.94-2.04	140,240,320,460,520,700	2.0-4.5

calibration plate and the nozzle was adjusted to ensure the droplet fell along the focal plane, which allowed the camera to capture the clear gas-liquid interface. The images were recorded at a frame rate of 10,000 fps with a resolution of 1,024×1,024 pixels. The maximum physical length per pixel was 0.02 mm and the boundary detection error was controlled below ±2 pixels. The laser-induced fluorescence (LIF) was applied in this study to further detect the liquids interaction. Rhodamine B was added to the fluid (mass concentration of 0.1 wt%) which can be induced by the sheet laser with 532 nm (MGL-F-532nm-2W, Beiting Measurement Technology (Beijing) Co., Ltd.), then the fluorescence was captured by the camera with a filter.

A stainless steel plate with size of 150 mm × 150 mm coated with a hydrophilic layer was used to support the liquid film. The liquid film thickness was detected by a chromatic confocal displacing sensor with a precision of 0.3 μm (ACR-HNDS100, Shanghai Dallas Optoelectronic Technology Co., Ltd), and the monitoring point was located 20 mm away from the droplet impact point. The liquid film thicknesses varied from 120 to 700 μm. The droplet produced by micro-syringe had a diameter d_0 of 1.99 ± 0.05 mm. The dimensionless liquid film thickness δ was defined as the ratio of the liquid film thickness h to the initial droplet diameter d_0. The experimental ranges are

Table 2 Physical properties of experimental fluids at 25°C

C_m, wt%	ρ, kg/m^3	μ, mPa·s	σ, N/m
0 (water)	1,000	0.9	0.0719
30	1,070	2.2	0.0665
60	1,150	8.8	0.0647
80	1,210	45.9	0.0634
100	1,258	905.6	0.0630

listed in Table 1. Table 2 shows the physical properties of water, glycerol and three glycerol aqueous solutions mass concentrations of 30 wt%, 60 wt% and 80 wt% at an ambient temperature of 25°C. All the experiments were carried out more than three times to ensure the repeatability.

3. ORIGIN OF SPLASHING FLUIDS

When a droplet impacts a liquid film of a different but miscible fluid, an interface is immediately formed at the moment of initial contact. Due to the short contact time, solute diffusion does not occur significantly, but the contrasting properties of the two fluids can influence the morphology of splashing. Therefore, identifying the origin of the splashing fluid is crucial to further study droplet impact on dissimilar liquid films. The planar laser-induced fluorescence (PLIF) technique, which entails adding fluorescent tracers in different fluids can be employed to discriminate the origin of the fluids. Figure 2 presents

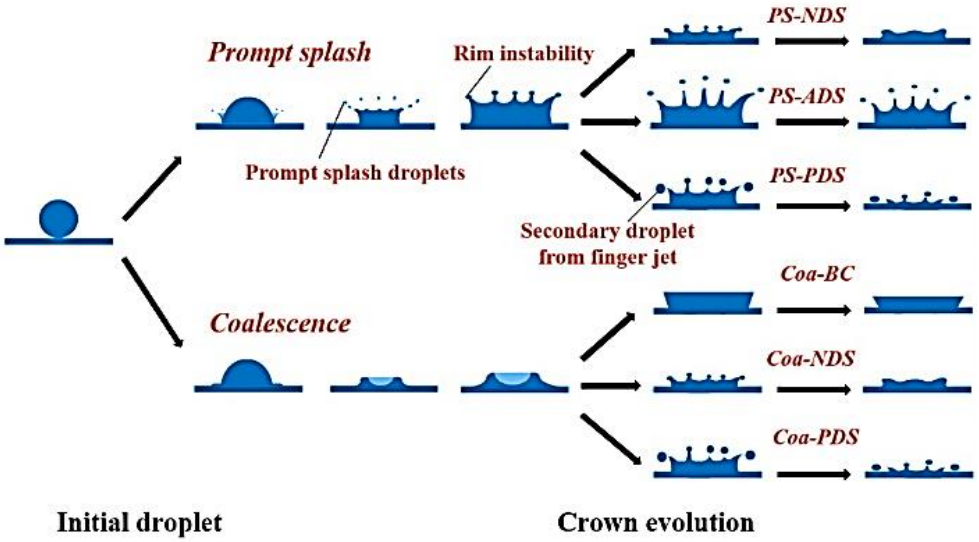

Fig. 3 Morphologies of a glycerol aqueous solution droplet impacting on a thin water film

three images: Fig.2 (a) is the fluorescent dye in the droplet, Fig. 2(b) is the fluorescent dye in the liquid film and Fig. 2(c) is captured using the backlighting method. Based on the comparisons of these images, it can be observed that the secondary droplets from prompt splash mainly originated from the liquid film, as mentioned by Uchida et al. (2015). In Fig. 2(a) and (b), the histograms illustrate the average gray value as a function of the X coordinate, corresponding to the horizontal position of the crown and reflecting the fluorescent concentration through brightness. The crown lamella in the two PLIF images both exhibit relatively high grayscale values, indicating that the crown lamella is composed of both liquid film and droplets. Two prominent peaks can be seen around the X coordinates 50 and 250 in both conditions. Furthermore, a broader high grayscale band of crown lamella is observed in the image where a fluorescent dye was added to the liquid film, with higher grayscale values compared with the image with the fluorescent dye added to the droplet. This suggests that the crown lamella is predominantly derived from the liquid film (Josserand et al., 2016; Che & Matar, 2018).

4. MORPHOLOGY CLASSIFICATION

In this experimental range, the splash also can be classified into *Prompt splash* (PS) and *Coalescence* (Coa), similar to the finding in the previous study (Zhu et al., 2021). However, due to the increased viscosity of the droplet, the impact behavior of a droplet on thin water films differs from that of water droplet, as illustrated in Fig. 3. The arrows in this figure indicate the potential evolutionary direction of phenomenon development. The *Prompt splash* can develop into three sub-regimes before the crown fully collapses: *Prompt splash without delayed splash* (PS-NDS), *Prompt splash with active delayed splash* (PS-ADS) and *Prompt splash with passive delayed splash* (PS-PDS). The first sub-regime presents a phenomenon that prompt splash secondary droplets are generated when the droplet initially impacts on the liquid film, but that no finger secondary droplets form in the subsequent process, as shown in Fig. 4(a). The second and third sub-regimes refer to prompt splash secondary droplets generated when the droplet initially impacts on the liquid film, followed by a delayed splash when the crown collapses, as shown in Fig. 4(b) and Fig. 4(c). The *Coalescence* may evolve into three possible subsequent regimes: *Coalescence Bowl-shaped crown* (Coa-BC), *Coalescence without delayed splash* (Coa-NDS), *Coalescence with passive delayed splash* (Coa-PDS). It should be mentioned that the Coa-BC denotes the phenomenon where the crown maintains its stability without rim instability from its formation to its collapse, as shown in Fig. 4(d). Figure 4(e) and (f) illustrate a crown with fingers (Coa-NDS) and delayed splash (Coa-PDS) after a no prompt splash impact, respectively. All the morphologies are shown in supplementary material S1~S6.

A map covering all regimes in this experiment is shown in Fig. 5 based on *We*, δ, and C_m. Obviously, the splash morphologies exhibited significant variation among different concentrations depicted in the splash regime map, indicating that viscosity exerts a profound influence on splash morphology. Generally, differently from the impact on a water film, the prompt splash with active delayed splash is not observed in this *We* and δ range. At C_m=80 wt%, no prompt splash occurs even when *We* reaches nearly 800. *Bowl-shaped crown* only occurs under higher viscosity (C_m=60 wt% and C_m=80 wt%) and smaller *We* (<300). Interestingly, the passive delayed splash tends to appear at C_m=60 wt%, namely, the crown finger breakup is more easily occur at C_m=60 wt%. Also, splash morphology seems to be insensitive to film thickness when *We* is smaller than 300.

To describe the influence of dynamic viscosity difference between droplet and film on splashing, we introduced the viscosity ratio,

$$\kappa=\mu_f/\mu_d \tag{1}$$

The dimensionless number K^* was used to determine the splash threshold (Kittel et al., 2017, 2018),

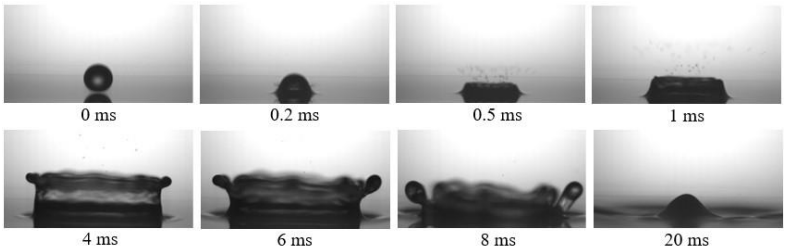

(a) PS-NDS (C_m=30 wt%, δ=0.16 and *We*=455)

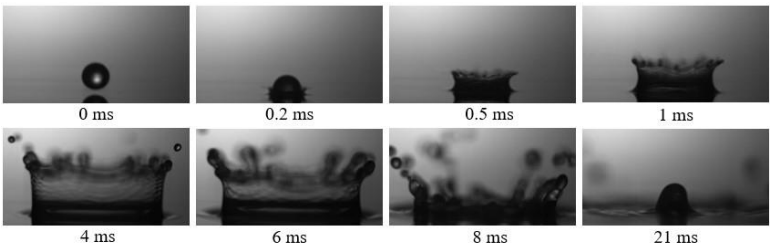

(b) PS-ADS (C_m=30 wt%, δ=0.16 and *We*=652)

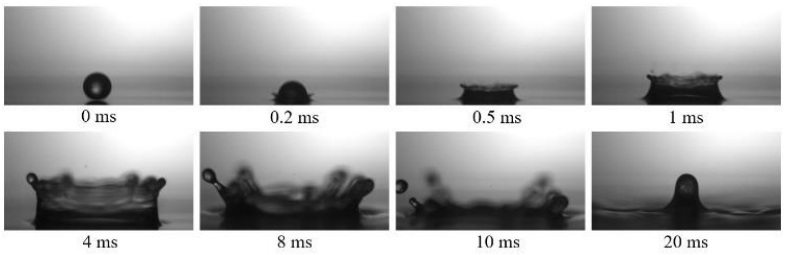

(c) PS-PDS (C_m=60 wt%, δ=0.23 and *We*=385)

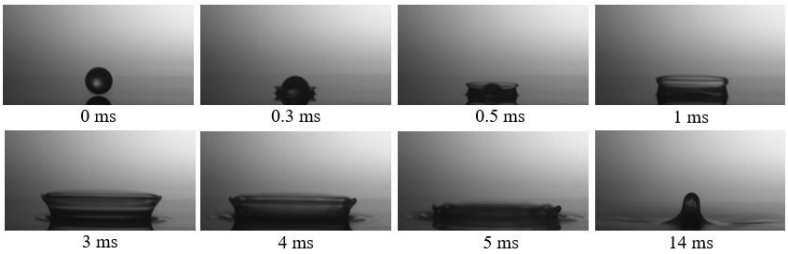

(d) Coa-BC (C_m = 60 wt%, δ=0.16 and *We*=269)

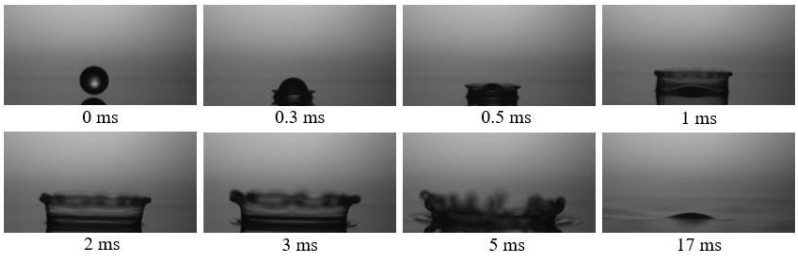

(e) Coa-NDS (C_m = 60 wt%, δ=0.12 and *We*=269)

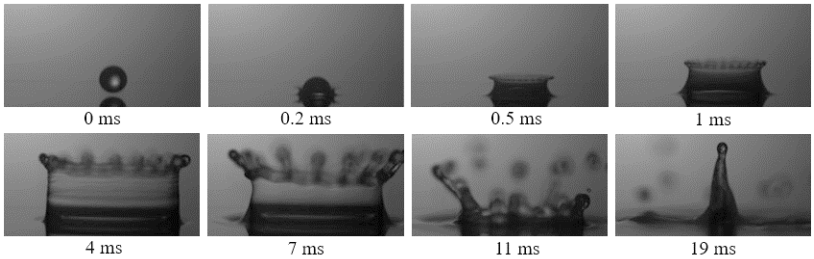

(f) Coa-PDS (C_m= 80 wt%, δ=0.23 and *We*=770)

Fig. 4 Typical morphologies

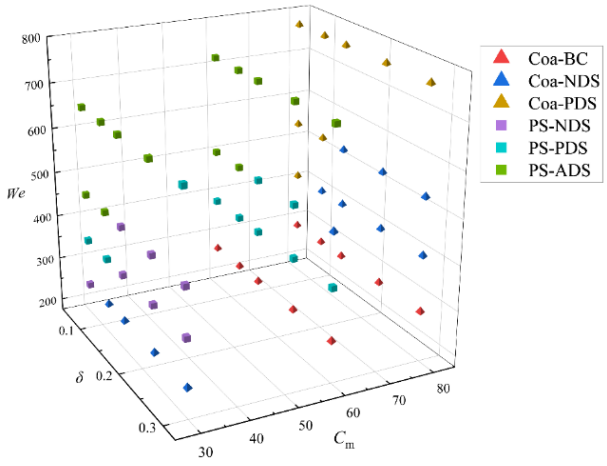

Fig. 5 Splash regimes based on *We*, *δ* and C_m

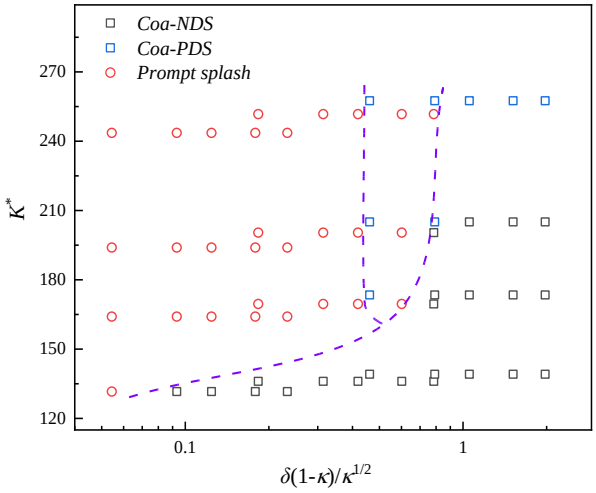

Fig. 6 Prompt splash/coalescence threshold

$$K^* = Re_d^{1/4} We^{*1/2} \tag{2}$$

Since the densities of two liquids in the experiments were comparable, the average density was used to calculate the equivalent Weber number We^*,

$$We^* = \frac{((\rho_f + \rho_d) d_0 v^2}{2min\{\sigma_d; \sigma_f\}} \tag{3}$$

The impact produces a composite crown of water and glycerol solution. An interface between the droplet and thin liquid film, which disappears during impact owing to miscibility. This mixing will enhance the energy transfer and reduce the motion discontinuity between the droplet and the thin liquid film. The boundary between coalescence and prompt splash can be clearly distinguished in the morphology map with K^* correlated of *δ* and *κ* in Fig. 6.

5. EFFECT OF DROPLET VISCOSITY

Figures 7 and 8 show the effects of droplet viscosity on crown sizes (crown upper diameter and height) and crown morphologies under *δ*=0.16, *v*=3.75 m/s, respectively.

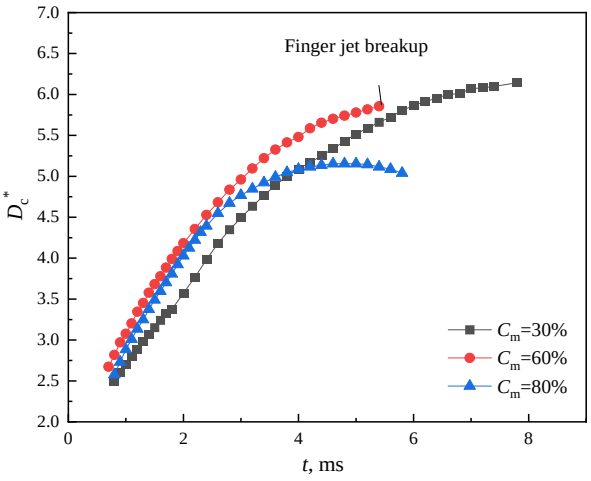

(a)

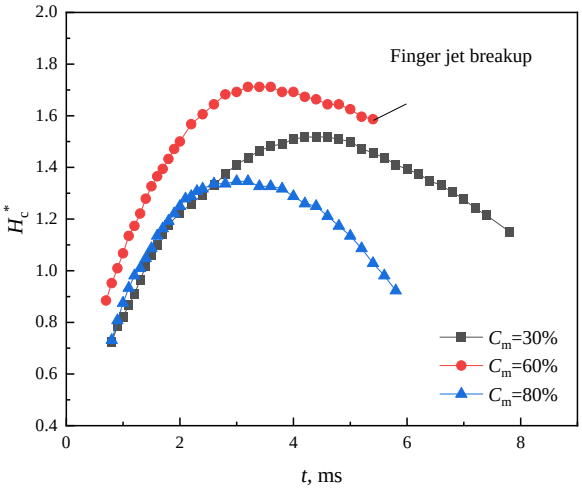

(b)

Fig. 7 Influence of droplet viscosity on crown evolution (*δ*=0.16, *v*=3.75 m/s)

The influence mechanism of viscosity on splash behavior is highly complex, as evident from Fig. 5, where each concentration map contains distinct splashing patterns. The curves in Fig. 7 also appear to lack regularity, however, combined with Fig. 8, these phenomena are evidently a result of the influence of viscosity. First, it can be confirmed that an increase in droplet viscosity leads to an earlier occurrence of its maximum height and diameter of the crown. Second, the increasing viscosity results in smoother crown rim and thinner crown lamella. Third, both the prompt splash and delayed splash are depressed by higher viscosity; therefore, the prompt splash rarely be found with a droplet of C_m=60 wt% and 80 wt%, while active delayed splash is not observed with a droplet of C_m=80 wt%.

At C_m=30 wt%, a prompt splash occurs at the moment of droplet impact, the expansion of crown is postponed and the crown diameter is smaller than that of the other two concentrations in the early stage of crown evolution, as shown in Fig. 8(a). The lower viscosity increases the crown diameter and delays the time needed to reach the maximum crown height. The crown lamella

(a) C_m=30 wt%, δ=0.12 and *We*=348

(b) C_m=60 wt%, δ=0.12 and *We*=385

(c) C_m=80 wt%, δ=0.12 and *We*=411

Fig. 8 Influence of droplet viscosity on crown morphology

of C_m=60 wt% has the maximum crown height when the crown expands along the radial direction. The moderate viscosity promotes the vertical development of the crown profile to, thereby enabling moderately thick lamella to achieve greater height. This crown evolution may have been caused by the shear effect between the droplet and liquid film. In Section 3, we observed that the crown crater bottom is entirely formed from the droplet. Hence, the increasing viscosity has a more direct influence on the crown base expansion compared with the crown diameter due to the larger resistance. The crown with C_m=80 wt% reaches its maximum diameter and height first since the crown expansion is inhibited by viscous dissipation enhancement.

6. EFFECT OF FILM THICKNESS

From Fig. 5, it can be found that the coalescence and prompt splash morphology do not change with variation of liquid film thickness; namely, the generation of secondary droplets from initial impact is independent of film thickness. However, the delayed splash generated from the crown is closely related to film thickness, the decreasing film thickness induces the secondary droplets separated from fingers when the crown collapses.

Figure 9 presents a typical quantitative evolution of the crown when a glycerol aqueous droplet impacts water film with C_m=80 wt% and *We*=537. Generally, the increase in liquid film thickness leads to a decrease in the expansion rate of the crown, since the increasing film enhances the flow resistance. It is interesting that the crown expansions with thinner film thickness (δ=0.07, 0.12, and 0.16) show a different evolution way compared with δ=0.23. Our previous studies indicated that the surface characteristics can influence the crown spreading when the impacted film is extremely thin[21]. Therefore, based on the observation of crown profile development in this work, it is observed that the expansion rate at the base

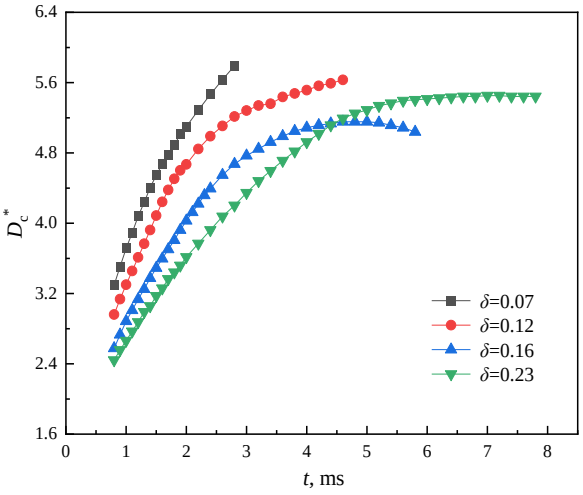

(a)

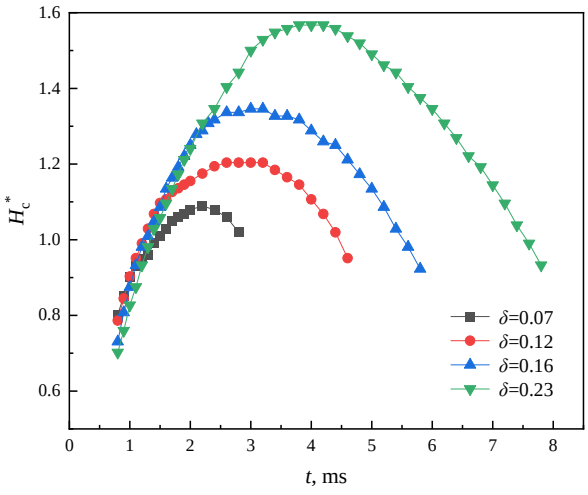

(b)

Fig. 9 Influence of film thickness on crown evolution (C_m= 80 wt%, *We*=537)

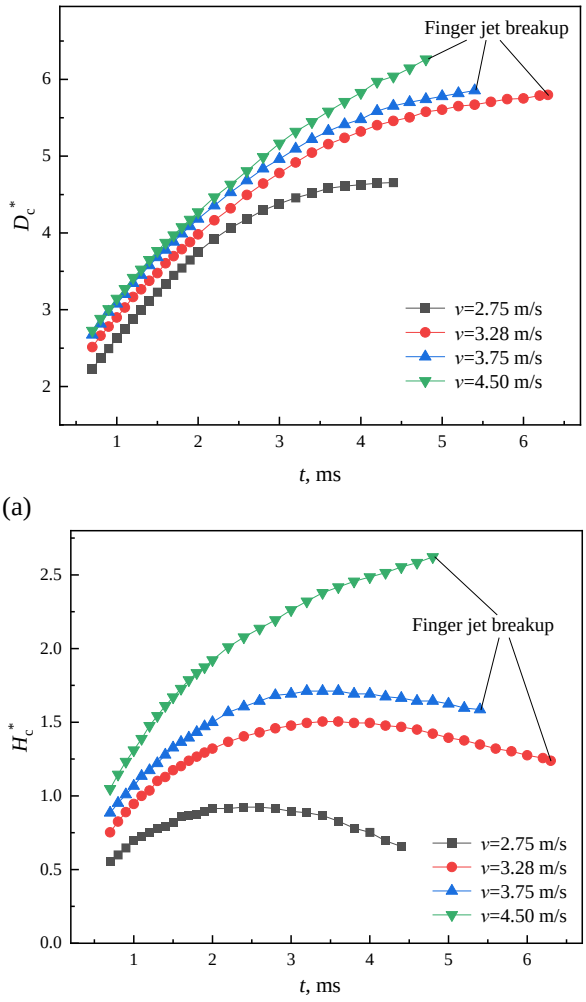

Fig. 10 Influence of impact velocity on crown evolution (C_m= 60 wt%, δ=0.16)

of the crown splash approaches that at the top of the crown splash when the dimensionless liquid film thickness reaches 0.24, thus slowing down the collapse of the crown lamella. However, in the case of impacting a thinner liquid film, it can be observed that the expansion at the base of the crown splash is significantly delayed compared with the expansion at the top of the crown splash due to the influence of the surface. Therefore, the greater stretching of the crown lamella resulted from thinner liquid films make passive delayed splashing more likely to occur; in contrast, passive delayed splashing is inhibited.

The initial rising rate of the crown is unaffected by the liquid film thickness. However, with increasing liquid film thickness, the maximum height of the crown increases. This is because a thicker liquid film constrains the radial expansion of the crown, resulting in a more pronounced transfer of kinetic energy to the upward motion of the crown evolution.

7. EFFECT OF IMPACT VELOCITY

Figure 10 shows that the impact of a C_m=60 wt% glycerol aqueous droplet on a δ=0.16 liquid film at different velocities. It is found that the crown diameter and height increase with increasing impact velocity. The

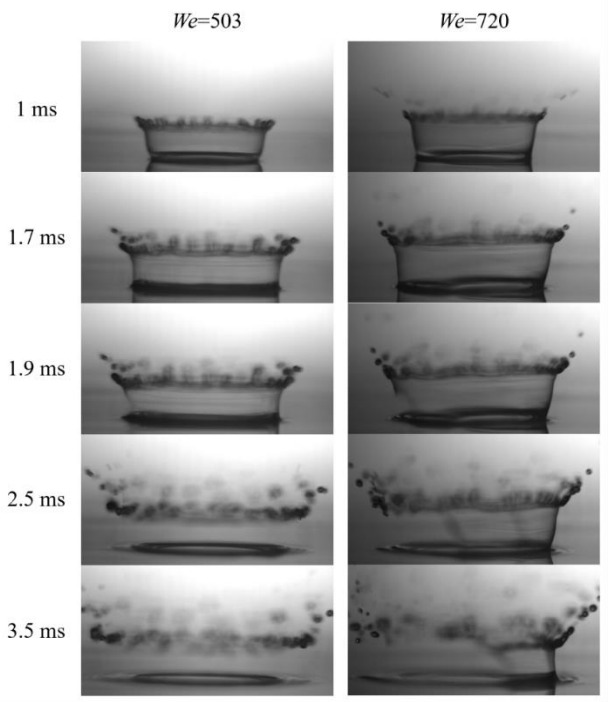

Fig. 11 Crown lamella rupture (C_m= 60 wt%, δ=0.07)

reason is that with the increase of impact velocity, the momentum of the crown increases. Increasing impact velocity creates more rim instability in the crown, making the splash more drastic. With the increase of impact velocity, the regime of splash transforms from the bowl-shaped crown to PS-PDS. When v=4.50 m/s, secondary droplets pinch-off during the crown expansion process as fingers shrink due to surface tension. However, when v=3.28 m/s and v=3.75 m/s, secondary droplets do not breakup from the finger jet until the crown collapse.

8. CROWN LAMELLA RUPTURE PHENOMENON

A series of interesting experimental images of a glycerol aqueous droplet impacting onto extremely thin water film are captured and shown in Fig. 11. The crown evolves after impact with thinner crown wall and the prompt splash occurs violently when the crown is still expanding. The crown bottom detaches from the water film at 1.9 ms and retracts to crown upper rim quickly (less than 2 ms). The crown lamella breaks into numerous tiny secondary droplets as soon as the moving crevasse “sweeps” across the crown. The crown lamella rupture process after impacting C_m=60 wt%, δ=0.07 is shown in supplementary material S7. This phenomenon only occurs at We≥503 and thin film thickness δ≤0.12 with C_m=60 wt% in this experiment. The occurrence of this phenomenon requires not only the proper viscosity ratio between droplet to liquid film, but also appropriately the thin pre-existing film and an impact velocity large enough to ensure sufficient kinetic energy to stretch the lamella. Lamanna et al. (2022) and Stumpf et al. (2023) pointed out that metastable zones formed in the very thin crown lamella can be triggered by small disturbance, which causes the rupture of the lamella and the creation of a web-like structure. Then the lamella rapidly ruptured by

Taylor-Culick velocity since it is significantly larger than the local flow velocity in the lamella.

9. CONCLUSION

The behaviors of glycerol aqueous droplet impacting on thin water film were studied experimentally. The crown morphology and evolution phenomena were analyzed under various droplet viscosity, film thickness and impact velocity. The PLIF experiment was employed to ascertain the origin of the crown by adding florescence dye in droplet and liquid film, respectively.

The crown morphologies observed in this experiment are categorized into six regimes and depicted in a morphology map based on We, δ and C_m. A threshold between *Prompt splash* and *Coalescence* is presented in the κ– δ image.

In the presence of rising droplet viscosity, both the maximum height and maximum diameter of the crown manifest at earlier stage. As the liquid film thickness increases, the crown expansion rate decreases while the maximum crown height increases. Additionally, both the maximum crown diameter and maximum crown height increase with increasing impact velocity. Crown lamella rupture is observed under specific conditions, requiring a larger impact velocity, extremely thin liquid film and appropriate viscosity.

ACKNOWLEDGEMENTS

The authors acknowledge financial support from the National Natural Science Foundation of China (No. 52076009).

CONFLICT OF INTEREST

The authors declare that they have no known competing financial interests or personal relationships that could have appeared to influence the work reported in this paper.

AUTHORS CONTRIBUTION

Jiamin Zhu: Investigation, Writing –original draft. **Bo Liu**: Investigation. **Jiang Sheng**: Methodology. **Shaowei Zheng**: Data curation. **Tao Lu**: Conceptualization. **Xue Chen**: Resources, Supervision, Conceptualization, Writing – review & editing.

SUPPLEMENTARY MATERIAL

S1 Coa-BC
S2 Coa-NDS
S3 Coa-PDS
S4 PS-ADS
S5 PS-NDS
S6 PS-PDS
S7 Crown lamella rupture

REFERENCES

Bernard, R., Baumgartner, D., Brenn, G., Planchette, C., Weigand, B., & Lamanna, G. (2020). Miscibility and wettability: how interfacial tension influences droplet impact onto thin wall films. *Journal of Fluid Mechanics*, *908*, A36. https://doi.org/10.1017/jfm.2020.944

Che, Z., & Matar, O. K. (2018). Impact of droplets on immiscible liquid films. *Soft Matter*, *14*(9), 1540-1551. https://doi.org/10.1039/C7SM02089A

Chen, N., Chen, H., & Amirfazli, A. (2017). Drop impact onto a thin film: Miscibility effect. *Physics of Fluids*, *29*(9), 092106. https://doi.org/10.1063/1.5001743

Cossali, G. E., Coghe, A. & Marengo, M. (1997). The impact of a single drop on a wetted solid surface. *Experimental in Fluids*, *22(6)*, 463-472. https://doi.org/10.1007/s003480050073

Cossali, G. E., Marengo, M., Coghe, A., & Zhdanov, S. (2004). The role of time in single drop splash on thin film. *Experiments in Fluids*, *36*(6), 888-900. https://doi.org/10.1007/s00348-003-0772-0

Ersoy, N. E., & Eslamian, M. (2019). Capillary surface wave formation and mixing of miscible liquids during droplet impact onto a liquid film. *Physics of Fluids*, *31*(1), 012107. https://doi.org/10.1063/1.5064640

Ersoy, N. E., & Eslamian, M. (2020). Phenomenological study and comparison of droplet impact dynamics on a dry surface, thin liquid film, liquid film and shallow pool. *Experimental Thermal and Fluid Science*, *112*, 109977. https://doi.org/10.1016/j.expthermflusci.2019.109977

Geppert, A., Terzis, A., Lamanna, G., Marengo, M., & Weigand, B. (2017). A benchmark study for the crown-type splashing dynamics of one- and two-component droplet wall–film interactions. *Experiments in Fluids*, *58*, 172. https://doi.org/10.1007/s00348-017-2447-2

Guo, J., Dai, S., & Dai, Q. (2010). Experimental research on the droplet impacting on the liquid film. *Acta Physica Sinica*, *59(04)*, 2601-2609. https://wulixb.iphy.ac.cn/en/article/doi/10.7498/aps.59.2601

Guo, Y., Lian, Y., & Sussman, M. (2016). Investigation of drop impact on dry and wet surfaces with consideration of surrounding air. *Physics of Fluids*, *28*(7), 073303. https://doi.org/10.1063/1.4958694

Guo, Y., Wei, L., Liang, G., & Shen, S. (2014). Simulation of droplet impact on liquid film with CLSVOF. *International Communications in Heat and Mass Transfer*, *53*, 26-33. https://doi.org/10.1016/j.icheatmasstransfer.2014.02.006

Josserand, C., Ray, P., & Zaleski, S. (2016). Droplet impact on a thin liquid film: anatomy of the splash.

Journal of Fluid Mechanics, *802*, 775-805. https://doi.org/10.1017/jfm.2016.468

Kittel, H. M., Roisman, I. V., & Tropea, C. (2017, September 6-8). *Splashing of a very viscous liquid drop impacting onto a solid wall wetted by another liquid*. ILASS-Europe 2017. 28th Conference on Liquid Atomization and Spray Systems, Valencia, Spain. https://pdfs.semanticscholar.org/585c/ece6d57800d94226d3babee63728f50b702f.pdf

Kittel, H. M., Roisman, I. V., & Tropea, C. (2018). Splash of a drop impacting onto a solid substrate wetted by a thin film of another liquid. *Physical Review Fluids*, *3* , 073601. https://doi.org/10.1103/PhysRevFluids.3.073601

Lamanna, G., Geppert, A., Bernard, R., & Weigand, B. (2022). Drop impact onto wetted walls: an unsteady analytical solution for modelling crown spreading. *Journal of Fluid Mechanics*, *938*, A34. https://doi.org/10.1017/jfm.2022.69

Lee, J. B., & Lee, S. H. (2011). Dynamic wetting and spreading characteristics of a liquid droplet impinging on hydrophobic textured surfaces. *Langmuir*, *27*(11), 65-73. https://doi.org/10.1021/la104829x

Liang, G., Guo, Y., Shen, S., & Yang, Y. (2013). Crown behavior and bubble entrainment during a drop impact on a liquid film. *Theoretical and Computational Fluid Dynamics*, *28*(2), 159-170. https://doi.org/10.1007/s00162-013-0308-z

Liang, G., Li, L., Chen, L., Zhou, S., & Shen, S. (2021). Impact of droplet on flowing liquid film: Experimental and numerical determinations. *International Communications in Heat and Mass Transfer*, *126*, 105459. https://doi.org/10.1016/j.icheatmasstransfer.2021.105459

Manzello, S. L., & Yang, J. C. (2002). An experimental study of a water droplet impinging on a liquid surface. *Experiments in Fluids*, *32*(5), 580-589. https://doi.org/10.1007/s00348-001-0401-8

Motzkus, C., Gensdarmes, F., & Géhin, E. (2009). Parameter study of microdroplet formation by impact of millimetre-size droplets onto a liquid film. *Journal of Aerosol Science*, *40*(8), 680-692. https://doi.org/10.1016/j.jaerosci.2009.04.001

Nikolopoulos, N., Theodorakakos, A., & Bergeles, G. (2005). Normal impingement of a droplet onto a wall film: a numerical investigation. *International Journal of Heat and Fluid Flow*, *26*(1), 119-132. https://doi.org/10.1016/j.ijheatfluidflow.2004.06.002

Okawa, T., Kawai, K., Kubo, K., & Kitabayashi, S. (2022). Fundamental characteristics of secondary drops produced by early splash during single-drop impingement onto a thick liquid film. *Experimental Thermal and Fluid Science*, *131*, 110533. https://doi.org/10.1016/j.expthermflusci.2021.110533

Okawa, T., Kubo, K., Kawai, K., & Kitabayashi, S. (2021). Experiments on splashing thresholds during single-drop impact onto a quiescent liquid film. *Experimental Thermal and Fluid Science*, *121*. 110279. https://doi.org/10.1016/j.expthermflusci.2020.110279

Okawa, T., Shiraishi, T., & Mori, T. (2006). Production of secondary drops during the single water drop impact onto a plane water surface. *Experiments in Fluids*, *41*(6), 965-974. https://doi.org/10.1007/s00348-006-0214-x

Rioboo, R., Bauthier, C., Conti, J., Voue, M., & De Coninck, J. (2003). Experimental investigation of splash and crown formation during single drop impact on wetted surfaces. *Experiments in Fluids*, *35*(6), 648-652. https://doi.org/10.1007/s00348-003-0719-5

Shaikh, S., Toyofuku, G., Hoang, R., & Marston, J. O. (2018). Immiscible impact dynamics of droplets onto millimetric films. *Experiments in Fluids*, *59*(1), 7. https://doi.org/10.1007/s00348-017-2461-4

Stumpf, B., Roisman, I. V., Yarin, A. L., & Tropea, C. (2023). Drop impact onto a substrate wetted by another liquid: corona detachment from the wall film. *Journal of Fluid Mechanics*, *956*, A10. https://doi.org/10.1017/jfm.2022.1060

Thoroddsen, S., Etoh, T., & Takehara, K. (2006). Crown breakup by a thousand holes. *Physics of Fluids*, *18*, 091110. https://doi.org/10.1063/1.2336802

Uchida, R., Tanaka, D., Noda, T., Okamoto, S., Ozawa, K., & Ishima, T. (2015). Impingement behavior of fuel droplets on oil film. *SAE Technical Papers*, *01*, 0913. https://doi.org/10.4271/2015-01-0913

Vander Wal, R. L., Berger, G. M., & Mozes, S. D. (2005). Droplets splashing upon films of the same fluid of various depths. *Experiments in Fluids*, *40*(1), 33-52. https://doi.org/10.1007/s00348-005-0044-2

Wang, A. B., & Chen, C. C. (2000). Splashing impact of a single drop onto very thin liquid films. *Physics of Fluids*, *12(9)*, 2155-2158. https://doi.org/10.1063/1.1287511

Weiss, D. A., & Yarin, A. L. (1999). Single drop impact onto liquid films: neck distortion, jetting, tiny bubble entrainment, and crown formation. *Journal of Fluid Mechanics*, *385*, 229–254. https://doi.org/10.1017/S002211209800411X

Wu, Y., Wang, Q., & Zhao, C. Y. (2020). Three-Dimensional droplet splashing dynamics measurement with a stereoscopic shadowgraph system. *International Journal of Heat and Fluid Flow*, *83*, 108576. https://doi.org/10.1016/j.ijheatfluidflow.2020.108576

Yeganehdoust, F., Attarzadeh, R., Karimfazli, I., & Dolatabadi, A. (2020). A numerical analysis of air

entrapment during droplet impact on an immiscible liquid film. *International Journal of Multiphase Flow*, *124*, 103175. https://doi.org/10.1016/j.ijmultiphaseflow.2019.103175

Zhang, H., & Liu, Q. (2020). Numerical investigation on performance of moisture separator: Experimental validation, applications and new findings. *Annals of Nuclear Energy*, *142*, 107362. https://doi.org/10.1016/j.anucene.2020.107362

Zhu, J., Tu, C., Lu, T., Luo, Y., Zhang, K., & Chen, X. (2021). Behavior of a water droplet impacting a thin water film. *Experiments in Fluids*, *62*, 143. https://doi.org/10.1007/s00348-021-03245-0